

whereas the computed peak is more smeared out. A possible source of the discrepancy is that the experiments were done at a temperature of 85°K whereas Rahman's computer experiments were at 94.4°K. We have used Henshaw's neutron-diffraction measurements⁷ at 84°K for $[\langle a \rangle^2 / \langle a^2 \rangle]$ and $S(\kappa)$, but our results are not particularly sensitive to this quantity since the momentum transfer κ is not a rapidly varying function of the final neutron wavelength.

We have not chosen to interpret the inelastic peaks in terms of a dispersion relation for the cooperative modes since the location of the peak in κ and ω is quite sensitive to the way in which the data are plotted. In fact, if we plot $S(\kappa, \omega)$ as a function of ω for fixed κ , we get only a rather flat shoulder on the curve rather than a well-defined peak. Even this structure is not present, however, in $S_S(\kappa, \omega)$. Thus the molecular-dynamics calculations of Rahman support the neutron-scattering experiments in predicting an observable effect of collective motion in liquid argon. We still do not have any theoretical framework which al-

lows this motion to be quantitatively described in terms of any well-defined elementary excitations.

We would like to thank Dr. Peter Egelstaff and Dr. A. Rahman for helpful discussions and correspondence and also for communicating to us the results of Refs. 1 and 5 prior to publication.

†Work supported by U. S. Atomic Energy Commission under Contract No. AT(30-1)-3326.

*On leave from Atomic Energy Establishment Trombay, Bombay, India.

¹S. H. Chen et al., Phys. Letters 19, 269 (1965).

²B. A. Dasannacharya and K. R. Rao, Phys. Rev. 137, A417 (1965).

³N. Kroo et al., Inelastic Scattering of Neutrons (International Atomic Energy Agency, Vienna, 1965), Vol. II, p. 101.

⁴A. Rahman, Phys. Rev. 136, A405 (1964).

⁵B. R. A. Nijboer and A. Rahman, "Time Expansion of Correlation Functions and the Theory of Slow Neutron Scattering" (to be published).

⁶K. S. Singwi and A. Sjölander, Phys. Rev. 120, 1093 (1960).

⁷D. G. Henshaw, Phys. Rev. 105, 976 (1957).

EFFECT OF UNIAXIAL STRESS ON MAGNON SIDEBANDS IN MnF₂

R. E. Dietz, A. Missetich,* and H. J. Guggenheim

Bell Telephone Laboratories, Murray Hill, New Jersey

(Received 17 March 1966)

Recently, a sideband of an optical transition in the absorption spectrum of MnF₂ was identified as arising from the simultaneous creation of an exciton and a magnon.¹ In this paper we report wave functions for the excitons² and selection rules for the coupling of the excitons to the magnons, as derived from optical absorption measurements of crystals of MnF₂ stressed uniaxially along the 001 and 110 directions. The zero-stress spectrum of the transition ${}^6A_{1g} \rightarrow {}^4T_{1g}$ in MnF₂, as reported in Ref. 1, consists of two sharp weak magnetic dipole lines $E1$ (at 18 419.6 cm⁻¹) and $E2$ (at 18 436.6 cm⁻¹), and three broad, relatively intense electric dipole lines $\sigma 1$ (at 18 477.1 cm⁻²), $\sigma 2$ (at 18 485.3 cm⁻¹), and $\pi 1$ (at 18 460.8 cm⁻¹). The magnetic dipole lines are observed in σ polarization only, and were attributed in Ref. 1 to exciton transitions; the polarizations of the electric dipole lines are

indicated in their identifying symbols. One of these lines, $\sigma 1$, was identified in Ref. 1 as a magnon sideband of $E1$ by the similarity of the shape and temperature dependence of the peak frequency to previous measurements of the magnon spectrum by other techniques.

Our measurements show that [001] stress shifts $E1$, $\pi 1$, and $\sigma 1$ by the same amount, while shifting $E2$ and $\sigma 2$ by a much smaller amount. This result confirms the identification in Ref. 1 of $\sigma 1$ as a sideband of $E1$, and, in addition, indicates $\pi 1$ to be also a sideband of $E1$, and $\sigma 2$ a sideband of $E2$. These results are summarized on the left-hand side of Fig. 1.

Whereas [001] stress merely shifts the absorption lines without splitting them, [110] stress splits each line into two. This result is to be expected since [001] stress affects the two Mn sublattices in the same way, while [110] stress acts along an x direction³ of one sublattice

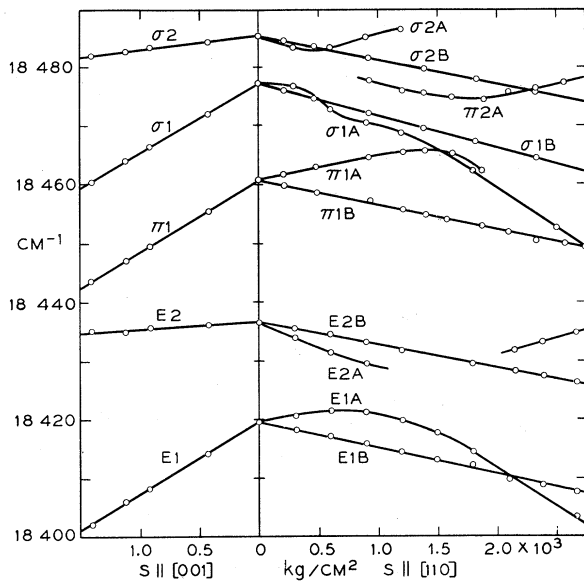


FIG. 1. Effect of [001] and [110] stress on the peak frequencies of absorption lines in MnF_2 at 1.5°K . All of the lines appear either in the σ ($E \perp [001]$, $k \parallel [110]$) or π ($E \parallel [001]$, $k \parallel [110]$) spectra except sidebands $\sigma 1B$ and $\sigma 2B$ which are seen only with $E \perp [001]$, $E \perp S$, $k \parallel [001]$. Notice that for sublattice *A*, all states deriving from exciton 1 interact strongly with those states deriving from exciton 2, while neither states on sublattice *B* nor those on different sublattices interact.

tice and along the y direction of the other, these directions being inequivalent for a single manganese site. Thus each of the lines produced by [110] stress is associated with a particular sublattice, say *A* or *B*.

If we examine the behavior of the exciton states $E1$ and $E2$ under [110] stress, we notice that two of the lines have a strong anticrossing, the minimum separation being about 8 cm^{-1} . Since we expect the interaction of excitons on the different, inequivalent sublattices to be small compared with the interaction of levels on the same sublattice, we label the anticrossing excitons as belonging to sublattice *A*: $E1A$ and $E2A$; and assign the other two excitons to sublattice *B*. There is no detectable repulsion between exciton levels on different sublattices.

Turning our attention to the sidebands, we find that each sideband can be associated with an exciton on a particular sublattice (although the magnon itself may propagate on the other sublattice); we further notice that anticrossings occur in both the π and σ bands, and there is some evidence for a level repulsion between $\sigma 1A$ and $\pi 2A$ at about 1000 kg/cm^2 .

In addition to the shifts and splittings of the zero-magnon lines and sidebands, there are changes in their strengths (the integrated absorption coefficient) with stress which are summarized in Figs. 2(a) and 3. The total area of the excitons is independent of stress within the estimated error of less than 10%. The same is true for σ and for π sidebands. The strength measurements correlate closely with the anticrossing effects and suggest that the sideband strengths can be simply related to the exciton wave functions.

In order to obtain those wave functions, we consider the matrix elements between the 12 basis functions $|M_L, M_S\rangle$ of 4T_1 (using the T_1 - p equivalence) of a Hamiltonian including spin-orbit interactions, tetragonal (Δ) and rhombic (Γ) distortions, and the exchange interaction in the form of an effective magnetic field (assuming the molecular-field model):

$$\mathcal{H} = \sum_i \xi L_i \cdot S_i + \Delta (L_x^2 - \frac{2}{3}) + \Gamma (L_y^2 - L_z^2) + H_{\text{eff}} S_z.$$

Since the spin-orbit interaction gives small

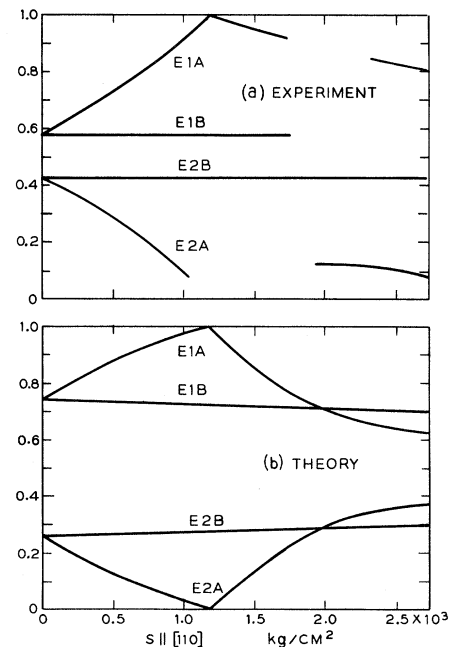


FIG. 2. Effect of [110] stress on the relative strengths of the zero-magnon lines. (a) gives the experimental relative strengths, while (b) shows the results of a calculation described in the text, using the energy separations of the excitons shown in Fig. 1. Part of the strength data of $E1A$ and $E1B$ are omitted since these excitons cross in that region so that one cannot assign separate strength values to them.

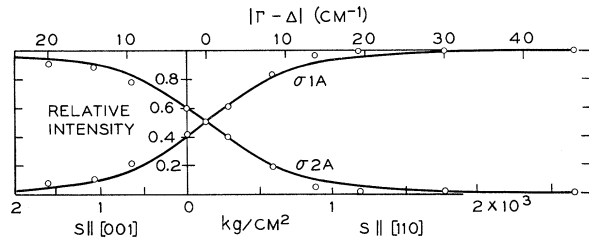


FIG. 3. Effect of [001] and [110] stress on the relative strengths of sidebands $\sigma 1A$ and $\sigma 2A$. The points are experimental and the curves are theoretical. The relative strengths were computed by setting $|\Gamma - \Delta| = 0$ at the anticrossing point, and computing values of $|\Gamma - \Delta|$ for other values of stress from the peak separations of $\sigma 1A$ and $\sigma 2A$. The abscissa is $|\Gamma - \Delta|$. It is observed that $|\Gamma - \Delta|$ is linear with the stress for both excitons and sidebands. This is considered good evidence that $|\Gamma - \Delta|$ vanishes at the anticrossing rather than assuming a minimum value. This conclusion is further verified by the fact that the intensity of $E 2A$ is zero at the anticrossing (see Fig. 2).

contributions (only second or higher order) and since we should observe⁴ in the $\sigma (H \parallel c)$ spectrum only transitions to $|1, \frac{3}{2}\rangle$, the 12×12 matrix can be approximately factored, retaining only the 2×2 matrix whose basis functions are $\Psi_1 = |1, \frac{3}{2}\rangle$ and $\Psi_{-1} = |-1, \frac{3}{2}\rangle$. The difference in energy between the resulting two levels is

$$\Delta E = [\alpha^2 + (\Gamma - \Delta)^2]^{1/2}, \quad (1)$$

where α is an empirical parameter for second-order spin-orbit contributions. The effect of pressure will be mainly to change Γ and Δ .⁵ The anticrossing point can then be understood as the position for which $\Gamma - \Delta = 0$. This permits us to determine α (about 8 cm^{-1}) from the minimum value observed for ΔE . We can then obtain the form of the basis functions of the excitons (except for the relative sign of c and c') where Ψ_- is the function for $E 1$, and Ψ_+ for $E 2$:

$$\Psi_+ = c\Psi_1 + c'\Psi_{-1}, \quad \Psi_- = c'\Psi_1 - c\Psi_{-1},$$

for any value of ΔE corresponding to a certain pressure, from the relation

$$\frac{c}{c'} = \frac{\Gamma - \Delta}{\alpha + \Delta E}. \quad (2)$$

For the zero-stress excitons, $|c| = 0.51$ and $|c'| = 0.86$. The g factors predicted for $E 1$ and $E 2$ using these values of the coefficients agree within the experimental error with the measurements reported in Ref. 4. The resulting

wave functions were then used to compute the strengths (assumed⁶ proportional to the square of the coefficient of Ψ_1) of the exciton lines [Fig. 2(b)] which are in reasonable agreement with the experimental values [Fig. 2(a)].

In order to interpret the magnon sidebands, we construct the following model: Since the sidebands of excitons on sublattice A have anticrossings at different values of stress than the zero-magnon excitons, but have similar energy splittings at the anticrossing, we suppose that the excitons which are created simultaneously with a magnon have values of $\Gamma - \Delta$ which are different from, and values of α which are similar to, the zero-magnon excitons. The difference in $\Gamma - \Delta$ (the absolute correction in $\Gamma - \Delta$ for both σ and π sidebands is about 12 cm^{-1} , but of opposite sign) may be due to the dispersion of the excitons, or to a change in the crystal-field parameters of the exciton due to the coupling between the magnon and the exciton. Since the strains induced by experiment were small relative to the inherent distortions from cubic symmetry, we assume that the zone-boundary magnon energy is independent of stress. These assumptions enable us to equate the sideband splittings to exciton splittings, and thus calculate wave functions as for the zero-magnon excitons.

However, it is clear from the experimental data in Figs. 2 and 3 that the sideband strengths are related to their exciton wave functions but not in the same way as are the strengths of the zero magnon lines. This is to be expected since the sidebands are electric dipole transitions which become allowed through the admixture of odd parity into the even-parity exciton states through interaction with the magnon.

For large energy separations of the two excitons on a given sublattice, that is, large $|\Gamma - \Delta|$, it is observed that in a given polarization one of the sidebands has the total of $1A$ and $2A$ sideband strength. For example, in Fig. 3, it is seen that $\sigma 1A$ has the entire strength for large values of [110] stress, whereas $\sigma 2A$ has the entire strength for large values of [001] stress where $\Gamma - \Delta$ has the opposite sign. For smaller values of $|\Gamma - \Delta|$, the intensity is transferred from one sideband to the other, the total intensity remaining constant. This indicates that one of the excitons for large $|\Gamma - \Delta|$ couples to the odd-parity states through the exciton-magnon interaction, while the other exciton

does not. For the condition of large $\Gamma-\Delta$ ($\Delta E \gg \alpha$), Eqs. (1) and (2) yield $\Psi_\sigma = (\Psi_1 \pm \Psi_{-1})/\sqrt{2}$ for the exciton wave function which couples to the magnons and its orthogonal function $\Psi_{\sigma \text{ orth}} = (\Psi_1 \mp \Psi_{-1})/\sqrt{2}$ for the exciton function which does not so couple.⁷ For the selection rule allowing the coupling of the excitons to the magnons in the π polarization, we have $\Psi_\pi = (\Psi_1 \mp \Psi_{-1})/\sqrt{2}$ since the intensity pattern is opposite to that of the σ sidebands. The effect of this selection rule is to cause $\pi 2A$ to vanish for [110] stress $< 1000 \text{ kg/cm}^2$; for the same reason $\pi 2B$ cannot be observed for feasible stresses.

To verify that these selection rules are valid for any value of $\Gamma-\Delta$, we computed the σ sideband strengths⁸ by taking $|\langle \Psi_\sigma | \Psi_- \rangle|^2$ proportional to the strength of the $\sigma 1A$ sideband, and $|\langle \Psi_\sigma | \Psi_+ \rangle|^2$ proportional to the strength of $\sigma 2A$. The wave functions of Ψ_+ and Ψ_- were computed for each value of the pressure from the energy difference between the magnon peaks. The results are shown as the curves in Fig. 3. Since the π sidebands are broad and overlap, we have not applied the same procedure to verify the Ψ_π selection rule in detail for intermediate values of $\Gamma-\Delta$.

Within the p equivalent representation, Ψ_σ and Ψ_π are p orbitals directed along [110], the directions for which the strongest superexchange interactions occur with the nearest Mn ions on the other sublattice.

The shapes of some of the sidebands are observed to change with stress, but, since the strengths of the sidebands appear to be related in a simple way to the exciton wave functions only, we leave consideration of the shapes to a future communication.

We are grateful for helpful discussions with J. J. Hopfield, G. F. Imbusch, L. F. Johnson, R. Loudon, M. D. Sturge, and L. R. Walker.

*With a fellowship of the Consejo Nacional de Investigaciones científicas y técnicas, Argentina.

¹R. L. Green, D. D. Sell, W. M. Yen, A. L. Schawlow,

and R. M. White, Phys. Rev. Letters **15**, 656 (1965).

²We follow the precedent established in Ref. 1 of referring to the zero-magnon states as "exciton" states. If, indeed, the excitations are delocalized, then the wave functions calculated in this paper should be considered to provide a basis for the excitons. The distinction between the localized and exciton descriptions is unimportant for the zero-magnon transitions which correspond to $k=0$ excitons. The exact significance of our basis for excitons coupling to zone-boundary magnons is not yet clear.

³See M. Tinkham, Proc. Roy. Soc. (London) **A236**, 549 (1956) for a definition of these coordinates.

⁴D. D. Sell, R. L. Green, W. M. Yen, A. L. Schawlow, and R. M. White, J. Appl. Phys. **37**, 1229 (1966).

⁵The downward trend of the observed levels for [110] stress may be due not only to changes in Γ and Δ , but also to changes in the cubic field parameters and the exchange field.

⁶As pointed out in Ref. 4, transitions are allowed only to excited states having the same M_J as the ground state.

⁷If we assume a second-order process, the electric dipole transition moment between the ground state of the crystal Ψ_G and the sideband state Ψ_{em} is

$$\langle \Psi_{em} | \vec{P} | \Psi_G \rangle = \sum_i \langle \Psi_{em} | \mathcal{K}_{em} | \Psi_i \rangle \langle \Psi_i | \vec{P} | \Psi_G \rangle / (E_i - E_{em}),$$

where Ψ_i is any excited state of odd parity and \mathcal{K}_{em} is the exciton-magnon interaction. Y. Tanabe, T. Moriya, and S. Sugano, Phys. Rev. Letters **15**, 1023 (1965), propose that \mathcal{K}_{em} may be the exchange operator. In weak coupling we can write

$$\Psi_{em} = \Psi_e \Psi_m,$$

where Ψ_m is the magnon state and Ψ_e the exciton,

$$\Psi_e = a \Psi_{\sigma \text{ or } \pi} \pm (1-a^2)^{1/2} \Psi_{(\sigma \text{ or } \pi) \text{ orth}}$$

The σ selection rules have the significance that

$$\sum_i \langle \Psi_{\sigma \text{ orth}} | \Psi_m | \mathcal{K}_{em} | \Psi_i \rangle \langle \Psi_i | \vec{P} | \Psi_G \rangle / (E_i - E_{em}) = 0,$$

$$\sum_i \langle \Psi_{\sigma} | \Psi_m | \mathcal{K}_{em} | \Psi_i \rangle \langle \Psi_i | \vec{P} | \Psi_G \rangle / (E_i - E_{em}) = \gamma,$$

where our experiment indicates that γ is independent of pressure. Similar relations hold for the π selection rules.

⁸Since Ψ_σ and $\Psi_{\sigma \text{ orth}}$ form a complete set of expanding Ψ_+ and Ψ_- , the strengths of the sidebands will simply be proportional to the square of the coefficient a of Ψ_σ in the expansion in Ref. 7.